

Calculation of binding energy using BLYP/MM for the HIV-1 integrase complexed with the S-1360 and two analogues

Cláudio N. Alves,^{a,*} Sergio Martí,^b Raquel Castillo,^b Juan Andrés,^b Vicent Moliner,^{b,*} Iñaki Tuñón^c and Estanislao Silla^{b,c}

^a*Departamento de Química, Centro de Ciências Exatas e Naturais, Universidade Federal do Pará, CP 11101, 66075-110 Belém, PA, Brazil*

^b*Departament de Química Física i Analítica, Universitat Jaume I, 12071 Castellón, Spain*

^c*Departament de Química Física, Universitat de Valencia, 46100 Burjassot, Valencia, Spain*

Received 19 January 2007; revised 26 February 2007; accepted 8 March 2007

Available online 13 March 2007

Abstract—Integrase (IN) is one of the three human immunodeficiency virus type 1 (HIV-1) enzymes essential for effective viral replication. S-1360 is a potent and selective inhibitor of HIV-1 IN. In this work, we have carried out molecular dynamics (MD) simulations using a hybrid Quantum Mechanics/Molecular Mechanics (QM/MM) approach, to determine the protein–ligand interaction energy for S-1360 and two analogues. Analysis of the MD trajectories reveals that the strongest protein–inhibitor interactions, observed in the three studied complexes, are established with Lys-159 residue and Mg²⁺ cation. Calculations of binding energy using BLYP/MM level of theory reveal that there is a direct relationship between this theoretical computed property and the experimental determined anti-HIV activity.

© 2007 Elsevier Ltd. All rights reserved.

1. Introduction

Human immunodeficiency virus type-1 integrase (HIV-1 IN) is an essential enzyme for effective viral replication. A number of compounds bearing a diketo acid (DKA) moiety with anti-HIV-1 IN activity have been independently discovered by scientists from Shionogi & Co., Ltd¹ and Merck Research Laboratories.² These compounds represent one of the most promising classes of HIV-1 IN inhibitors in terms of potency and selectivity. One of these compounds, S-1360, inhibits IN activity with an IC₅₀ value of 0.02 μM and was the first IN inhibitor to undergo clinical trials.³ However, S-1360 failed phase II clinical trial because of pharmacokinetic problems.³ All in all, S-1360 is a potent and selective IN inhibitor, and it should be possible to design molecules

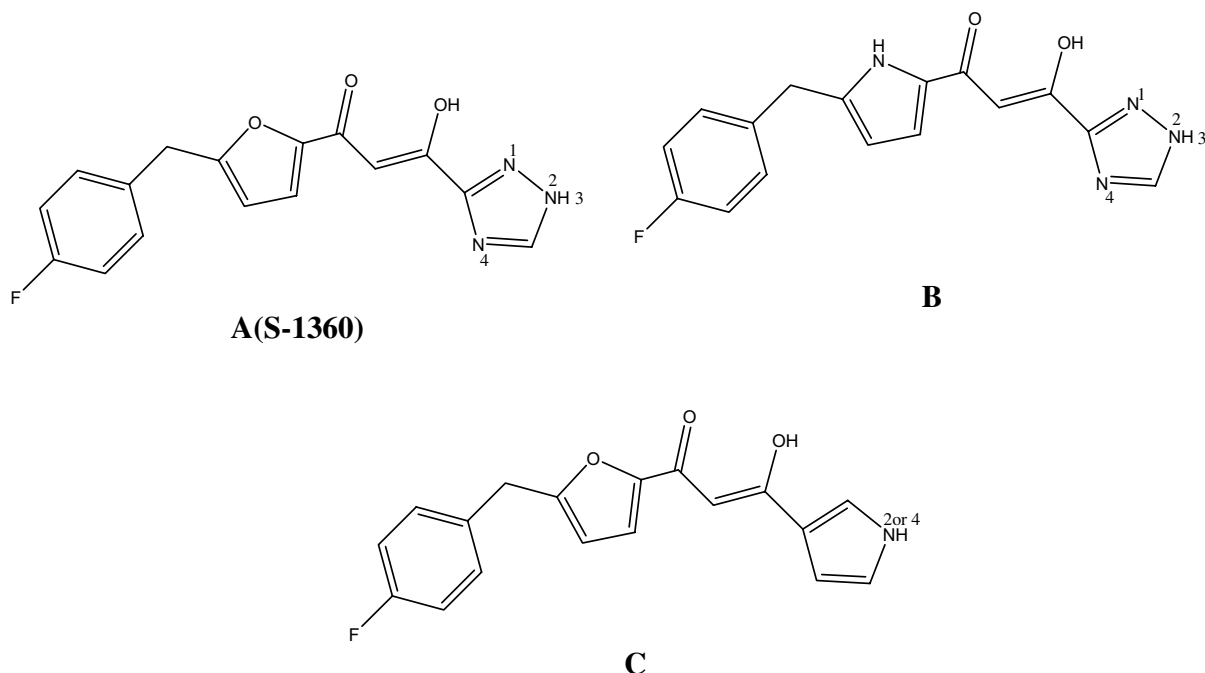
on the basis of its structure but with different pharmacokinetic properties.

Recently, an X-ray structure of one DKA analogue (5CITEP) has been crystallized with the enzyme,¹ it is a well-known bioisoster of a carboxylic acid.⁴ In this X-ray structure a single Mg²⁺ ion is chelated by Asp64, Asp116, and water molecules in an octahedral coordination. 5-CITEP and L-731,988 inhibitors have been also investigated by quantum chemical calculations,⁵ and Neamati and coworkers⁶ have reported docking studies of S-1360 inhibitor complexed with HIV-1 integrase (IN). Although, these and some other computational studies have been performed on DKA compounds, by means of classical molecular dynamics⁷ and docking⁸ studies, our understanding of the molecular mechanism is far from complete.

In this paper, we employed a combined quantum mechanical/molecular mechanical (QM/MM) approach^{9–11} to determine the protein–ligand interaction energy for S-1360 and two analogues acting as IN strand-transfer-selective inhibitor¹² (Scheme 1). Recently, we have successfully used this methodology to study the relationship between protein–ligand interaction energies and inhibitor activity for HIV-1 IN

Keywords: HIV-1; S-1360; Quantum mechanical/molecular mechanical (QM/MM); Molecular dynamics (MD); BLYP/MM; DFT; Binding energy.

* Corresponding authors at present address: Departament de Ciències Experimentals, Universitat Jaume I, 12071 Castellón, Spain. Tel.: +55 3201 1363; fax: +55 3201 1635 (C.N.A.); tel.: +34 964 728084; fax: +34 964 728066 (V.M.); e-mail addresses: nahum@ufpa.br; moliner@uji.es



Scheme 1. Structures and numbering of selected diketo acid-containing HIV-1 IN inhibitors.

activity,¹³ and Cyclin-Dependent Kinase 2 (CDK2).¹⁴ Following this strategy, a detailed analysis of the interactions of the three inhibitors mentioned above with the key residues inside the binding pocket is carried out. The results showed here can be used for making further design of more potent synthetic inhibitors with more appropriate features as putative anti-HIV-1 drugs.

2. Results and discussion

All QM/MM molecular dynamic calculations carried out in the present study were performed with the DYNAMO library.¹⁵ In all the calculations, the inhibitor has been treated with the semiempirical AM1 hamiltonian,¹⁶ while the rest of the system (protein plus water molecules) was described using the combination of the OPLS-AA¹⁷ and TIP3P¹⁸ force fields. Additionally, the final structures obtained from the 1 ns AM1/MM MD simulations have been optimized by means of Density Functional Theory (DFT)/MM methods.¹⁹ In particular, the BLYP functional²⁰ has been employed together with the 6-31G* basis set to describe the QM region of the system which includes, for these calculations, all atoms of the ligand plus the Mg^{2+} ion, while the OPLS-AA¹⁷ force field was used for the MM part. The protein–inhibitor interaction energy for the opti-

mized geometries is reported in Table 1 together with the IC_{50} values.

The optimized structures obtained from the BLYP/MM calculations are shown in Figure 1, while the contribution of individual residues to the total protein–substrate interaction energy is displayed in Figure 2. In this later figure, negative values correspond to stabilizing effects. Table 1 shows the values of the total ligand–protein interaction energies for these systems. In Figure 1, we can observe that the triazole ring of S-1360 interacts, through hydrogen bonds, with the pocket formed by Thr66, Asn155, Lys156, and Lys159 residues. These interactions favor the stabilization of the protein–inhibitor complex as can be observed in Figure 2. Another important residue is the Glu152, whose interaction with Lys156 residue stabilizes the cavity structure around the triazole ring of the inhibitor although, as observed, presents an unfavorable interaction with the ligand (a positive value). This could be probably the reason why Asn155 and Lys159 are critical for IN/DNA binding,²¹ as shown by mutagenesis^{21a–1c} and photo-cross-linking^{21d} studies. Both furan and benzene rings of the inhibitor interact with the Mg^{2+} cation, through an electrostatic attraction with the quadrupole moment created by the π electrons of the aromatic moiety, as previously suggested by Dougherty.²² This interaction is responsible for the aromatic rings to adopt an orientation in which the Mg^{2+} cation gets blocked. Moreover, it is similar to the one adopted by 5CITEP in the crystal structure¹ and Briggs et al.^{7f} found also the same orientation in the structure of inhibitor L-731,988 by using classical molecular dynamics and docking studies. The resulting conformation of the active site may be unable to perform integration reactions (see Fig. 3), as suggested by Pommier et al.²³ In addition, photo-cross-linking

Table 1. BLYP/MM Interaction energies and experimental measured anti-HIV IN activities obtained from Ref. 7

Compound	BLYP/MM (kJ/mol)	Activity (μ M)
A	–667.0	0.02
B	–611.7	<1
C	–622.7	<1

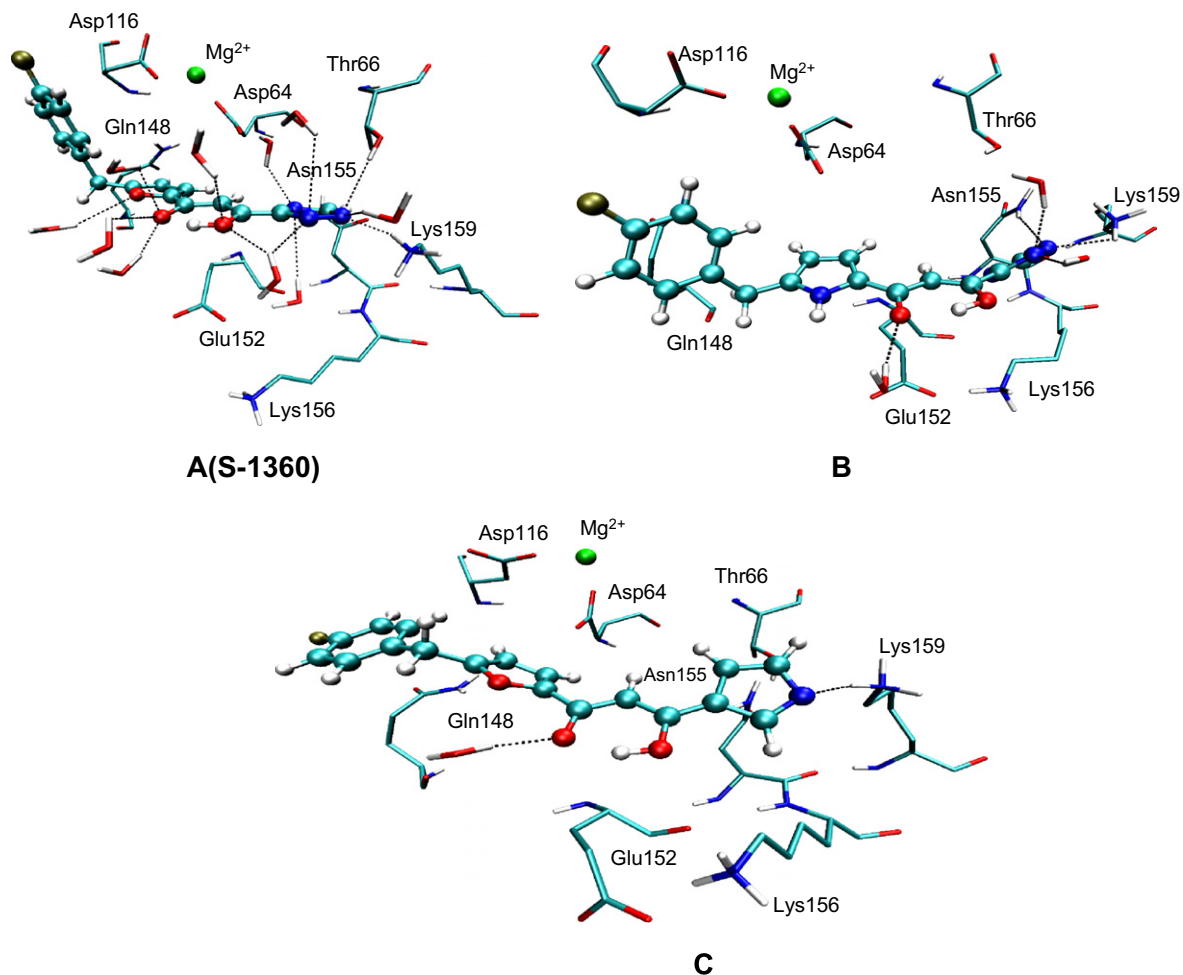


Figure 1. Representation of the most important interactions between the three HIV-1 IN inhibitors (A, B, and C), obtained from the BLYP/MM calculations.

studies^{21d} suggest that the conserved adenosine binding in the vicinity of Lys159 and Glu152, and the 5'-adenosine overhang should be in contact with Gln148. Finally, as observed in Figure 1, there are some water molecules that interact with the inhibitor stabilizing more the S-1360 complex, as deduced from Figure 2. McCammon et al.^{8a} and Briggs et al.^{7f} have found that water molecules are important in the stabilization of the L-731,988 and 5CITEP IN complex, in accordance with our theoretical simulations.

It is important to point out that, although compounds **B** and **C** present stronger interactions with Lys156 than S-1360, and significantly weaker unfavorable interactions with Asp64 and Glu152, it seems that interaction with Mg^{2+} cation is decisive in the total protein-ligand interaction (see Fig. 2 and Table 1). By comparison of these theoretical predicted data and the experimental measured anti-HIV activity (reported in Table 1), a direct relationship between both properties can be observed, which could be used as a guide in the design of new inhibitors.

The analysis of the averaged distances between the Mg^{2+} cation and the center of mass of the both benzene and

furan rings, obtained during the AM1/MM MD simulations, shows an increase along the series of inhibitors, from 5.85 and 5.34 Å in compound **A**, 6.40 and 7.05 Å in compound **B**, up to 7.80 and 6.74 Å in compound **C**. As suggested before, this tendency can be related to the lower activity and interaction energy (in absolute value) of compounds **B** and **C** with respect to **A** (see Table 1). Other interesting averaged distances of all the compounds are reported in Table 2. It can be observed how the N2 atom of inhibitors **A**, **B**, and **C** presents a strong hydrogen bond interaction with the side chain of Lys159; interaction that is reflected in Figure 2. Another conclusion derived from data reported in Table 2 is that, in general, AM1/MM renders longer protein-ligand distances than the BLYP/MM.

Recently, some computational studies performed with both DFT^{24a,b} and AM1 methods^{24c} have observed that the charges on some key atoms are important in QSAR studies of flavonoid compounds with anti-HIV activity. Moreover; previous QM/MM studies for other inhibitors confirm this hypothesis.¹³ Therefore, in this work we have also performed calculation of electronic density with the aim of understanding how structural changes can affect substrate charge distributions. Figure 4

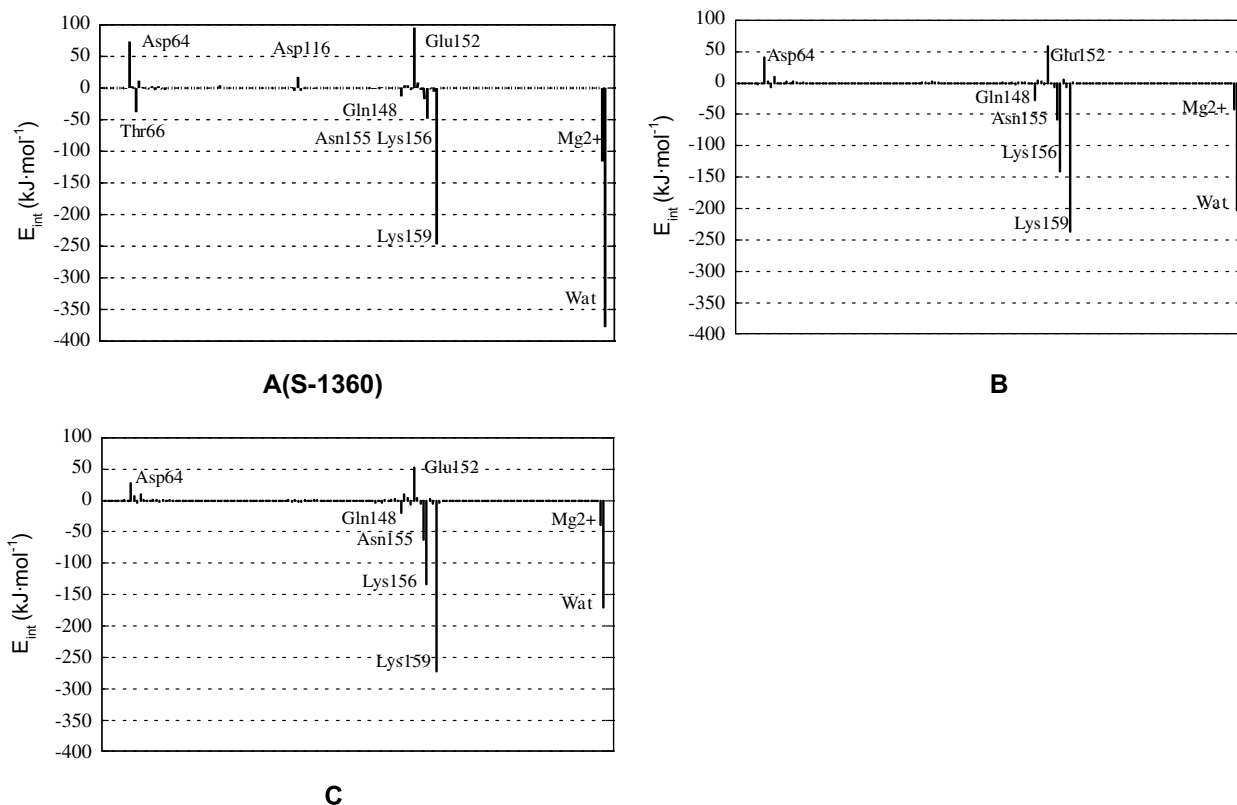


Figure 2. Contributions of individual amino acid residues to inhibitor binding (in $\text{kJ}\cdot\text{mol}^{-1}$) of the three inhibitors (A, B, and C) obtained by means of BLYP/MM method. Water refers to the effect of all the water molecules in the active site.

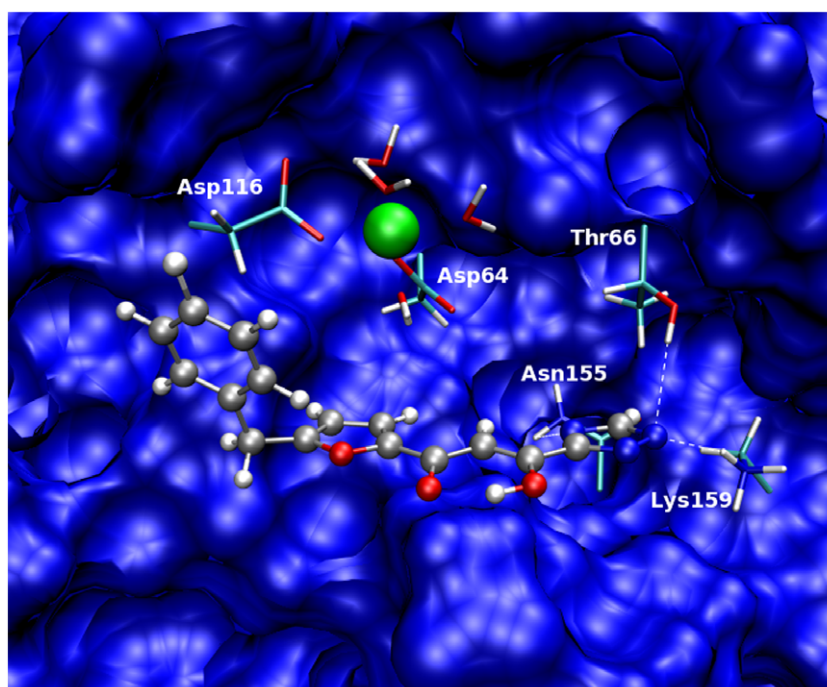


Figure 3. Representation of the orientation of the Mg^{2+} between HIV-1 IN and S-1360 inhibitor.

displays the three-dimensional molecular electrostatic potential (MEP) surfaces for the three compounds shown in Scheme 1. MEP surfaces were generated, with Gauss View program,²⁵ from the BLYP/MM optimized

structures. These surfaces correspond to an isodensity value of 0.002 au. The most nucleophilic regions (negative electronic potential) are shown in red, while the most electrophilic regions (positive electrostatic

Table 2. Averaged hydrogen-bond distances between the ligand and the hinge region of the integrase active site (in Å)

	A(S-1360)	B	C
(Lys159)NH3...N2(INH)	2.22 (± 0.36) [1.94]	2.05 (± 0.23) [2.40]	1.93 (± 0.18) [1.71]
(Thr66)O—H...N2(INH)	3.47 (± 0.52) [2.67]	—	—
(Asn155)C=O...H3(INH)	2.79 (± 0.24) [2.64]	—	—
(Asn155)N—H...N4(INH)	3.93 (± 0.40) [4.25]	2.89 (± 0.27) [2.61]	3.89 (± 0.37) [3.18]

The values in parentheses correspond to the standard deviations and values in bracket are for single molecule BLYP/MM calculations.

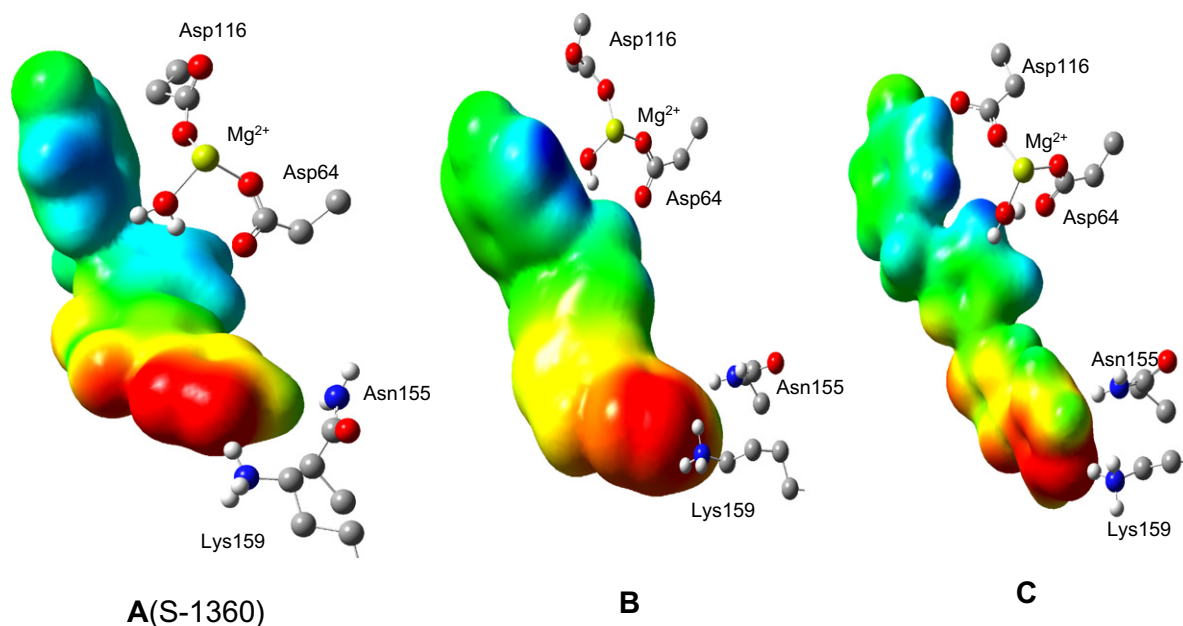


Figure 4. MEPS derived from BLYP(6-31G*)/MM calculations for the S-1360 inhibitor and the two analogues. The increase of negative charges comes from the blue (positive) to red (negative).

potential) are shown in blue. From Figure 4 we can observe a much more intense region of negative electrostatic potential around the triazole or pyridine ring, benzene ring, and keto-enol group. This observation can be related with the interactions established with the residues of the active site.

3. Conclusions

This work provides an insight into the activity of potential inhibitor against HIV-1 IN. Hybrid QM/MM MD calculations have been carried out for HIV-1 IN complexed with S-1360 and two analogues to determine the protein-ligand interaction energy. The interactions established between a putative HIV-1 IN inhibitor with Mg^{2+} , Asn155, Lys156 and Lys159, and water molecules seems to be crucial to determine its activity as anti-HIV drug. In particular, in the series of 3 compounds analyzed in this work, the cation–ligand interactions allow to rationalize the relative ordering in the inhibitor activity. Stronger interactions of compounds B and C with some residues of the active site, with respect to the S-1360, result in lower interaction energy because the averaged distance between the ligand and the cation is increased. These results might be useful to design compounds on the basis of its three-dimensional structure with more interesting anti-HIV-1 IN activity.

4. Methods

The initial structure was built from the A-chain of the X-ray crystal structure complexed with the 5CITEP inhibitor (1QS4).¹ This chain has been used as a starting point for all three inhibitors, just changing the substrate molecule by the different inhibitors depicted in Scheme 1. All the missing residues (141–144) were added using HYPERCHEM facility. Hydrogen atoms were placed in the protein according to the predicted pK_a of the amino-acids.²⁶ For this purpose, a statistical treatment of electrostatic potential calculations was performed, as implemented by Field and co-workers.²⁷ In this case, no unusual ionization states were found. For the inhibitor, due to the ability of the moiety to stabilize negative charges, all of them were modeled in a deprotonated form.

After adding the hydrogens to the structure, series of optimization algorithms (speest descent, conjugated gradient, and LBFGSB²⁸) were applied. In order to avoid a denaturalization of the protein structure, all the heavy atoms of the protein and the inhibitor were restrained by means of a Cartesian harmonic umbrella with a force constant of $1000 \text{ kJ}\cdot\text{mol}^{-1}\cdot\text{\AA}^{-2}$. Afterward the system was fully relaxed, but only restraining the peptidic backbone with a lower constant ($100 \text{ kJ}\cdot\text{mol}^{-1}\cdot\text{\AA}^{-2}$).

Then the optimized protein was placed in a cubic box of pre-equilibrated waters (80 Å side), using the principal axis of the protein-inhibitor complex as the geometrical center. Any water with an oxygen atom lying in a radius of 2.8 Å from a heavy atom of the protein was deleted. The remaining water molecules were then relaxed using optimization algorithms. Finally, 50 ps of hybrid QM/MM Langevin–Verlet molecular dynamics (NVT) at 300 K were used to equilibrate the model. For the hybrid QM/MM calculations, only the atoms of the inhibitor have been selected to be QM, using a semiempirical AM1 hamiltonian.¹⁶ The rest of the system (protein plus water molecules) was described using the OPLS-AA¹⁷ and TIP3P¹⁸ force fields, respectively, as implemented in the DYNAMO library.¹⁵

Due to amount of degrees of freedom, any residue 25 Å apart from any of the atoms of the initial inhibitor was selected to be kept frozen in the remaining calculations (10235 mobile atoms). Cutoffs for the non-bonding interactions were applied using a switching scheme, within a range of radius from 11 to 13 Å.

Afterward, each system was equilibrated by means of 900 ps of QM/MM MD at temperature of 300 K. The computed RMSD for the protein during the last 200 ps renders a value always below 0.9 Å. Furthermore, the RMS of the temperature along the different equilibration steps was always lower than 2.5 K and the variation coefficient of the potential energy during the dynamics simulations has been never higher than 0.3%.

On the other hand, in this paper we have made use of a BLYP(6-31G*)/OPLS-AA method, based on a semi-classical approach. The potential energy of our scheme is derived from the standard QM/MM formulation:

$$E_{\text{QM/MM}} = \langle \Psi | \hat{H}_o | \Psi \rangle + \left\langle \left\langle \Psi \left| \frac{q_{\text{MM}}}{r_{e,\text{MM}}} \right| \Psi \right\rangle \right\rangle + \sum \sum \frac{Z_{\text{QM}} q_{\text{MM}}}{r_{\text{QM,MM}}} + E_{\text{QM/MM}}^{\text{vdW}} + E_{\text{MM}} \quad (1)$$

$$E_{\text{QM/MM}} = E_{\text{vac}} + E_{\text{QM/MM}}^{\text{elect}} + E_{\text{QM/MM}}^{\text{vdW}} + E_{\text{MM}} \quad (2)$$

where E_{MM} is the energy of the MM subsystem terms, $E_{\text{QM/MM}}^{\text{vdW}}$ the van der Waals interaction energy between the QM and MM subsystems, and $E_{\text{QM/MM}}^{\text{elect}}$ includes both the coulombic interaction of the QM nuclei (Z_{QM}) and the electrostatic interaction of the polarized electronic wavefunction (Ψ) with the charges of the protein (q_{MM}). In order to take advantage of powerful optimization algorithms,^{19b} we have substituted the electrostatic interaction term by a pure coulombic one, in which the charges of the QM atoms are obtained by means of electrostatic potential fit methods based on the electronic density.²⁹ Thus, the final potential energy can be approximated by:

$$E_{\text{QM/MM}} = \langle \Psi | \hat{H}_o | \Psi \rangle + \sum \sum \frac{q_{\text{QM}}^{\text{ChelpG-fit}} q_{\text{MM}}}{r_{\text{QM,MM}}} + E_{\text{QM/MM}}^{\text{vdW}} + E_{\text{MM}} \quad (3)$$

Finally, the interaction energy between the inhibitor and the environment is evaluated as the difference between the QM/MM energy and the energies of the separated, non-interacting, QM and MM subsystems with the same geometry. Considering that the MM part is described using a non-polarizable potential the interaction energy is given by the following expression:

$$E_{\text{QM/MM}}^{\text{Int}} = \langle \Psi | \hat{H}_o | \Psi \rangle - \langle \Psi^o | \hat{H}_o | \Psi^o \rangle + \sum \sum \frac{q_{\text{QM}}^{\text{ChelpG-fit}} q_{\text{MM}}}{r_{\text{QM,MM}}} + E_{\text{QM/MM}}^{\text{vdW}} \quad (4)$$

where Ψ^o is the gas phase wavefunction of the inhibitor.

Acknowledgments

We thank DGI for project CTQ2006-15447-C02-01, Generalitat Valenciana for projects: GV06/016 and GV06/152, and Universitat Jaume I - BANCAIXA Foundation for projects P1-1B2005-13, P1-1B2005-15, and P1-1B2005-27 and the ‘Programa hispano-brasileño de cooperación interuniversitaria’ of the Spanish Ministry of Culture and Education for project CAPES N° 0014-13/05. Alves would like to thank CNPq for their financial support and the warm hospitality during the research stay at Departament de Ciències Experimentals, Universitat Jaume I. We are also grateful to Dr. M. Field and Dr. P. Amara for supporting us in the pK_a calculations and discussions. The authors also acknowledge the Servei d’Informàtica, Universitat Jaume I, for generous allotment of computer time.

References and notes

- Goldgur, Y.; Craigie, R.; Cohen, G. H.; Fujiwara, T.; Yoshinaga, T.; Fujishita, T.; Sugimoto, H.; Endo, T.; Murai, H.; Davies, D. R. *Proc. Natl. Acad. Sci. U.S.A.* **1999**, *96*, 13040–13043.
- Hazuda, D. J.; Felock, P.; Witmer, M.; Wolfe, A.; Stillmock, K.; Grobler, J. A.; Espeseth, A.; Gabryelski, L.; Schleif, W.; Blau, C.; Miller, M. D. *Science* **2000**, *287*, 646–650.
- Witvrouw, M.; Van Maele, B.; Vercammen, J.; Hantson, A.; Engelborghs, Y.; De Clercq, E.; Pannecouque, C.; Debyser, Z. *Curr. Drug Metab.* **2004**, *5*, 291–304.
- Herr, R. J. *Bioorg. Med. Chem.* **2002**, *10*, 3379–3393.
- Huang, M.; Richards, W. G.; Grant, G. H. *J. Phys. Chem. A* **2005**, *109*, 5198–5202.
- Dayam, R. L.; Neamati, N. *Bioorg. Med. Chem.* **2004**, *12*, 6371–6381.
- (a) Brigo, A.; Lee, K. W.; Mustata, G. I.; Briggs, J. M. *Biophys. J.* **2005**, *88*, 3072–3082; (b) Lee, M. C.; Deng, J.; Briggs, J. M.; Duan, Y. *Biophys. J.* **2005**, *88*, 3133–3146; (c) Barreca, M. L.; Lee, K. W.; Chimirri, A.; Briggs, J. M. *Biophys. J.* **2003**, *84*, 1450–1463; (d) Ni, H.; Sottriffer, C. A.; McCammon, J. A. *J. Med. Chem.* **2001**, *44*, 3043–3047; (e) Laboulasis, C.; Deprez, E.; Leh, H.; Mouscadet, J. F.; Brochon, J. C.; Bret, M. L. *Biophys. J.* **2001**, *81*, 473–489; (f) Brigo, A.; Lee, K. W.; Fologolari, F.; Mustata, G. I.; Briggs, J. M. *Proteins* **2005**, *59*, 723–741.
- (a) Sottriffer, C. A.; Ni, H.; McCammon, J. A. *J. Am. Chem. Soc.* **2000**, *122*, 6136–6137; (b) Beierlein, F.; Lanig, H.; Schurer, G.; Horn, A. H. C.; Clark, T. *Mol. Phys.*

- 2003, 101, 2469–2480; (c) Schames, J. R.; Henchman, R. H.; Siegel, J. S.; Sotriffer, C. A.; Ni, H.; McCammon, J. A. *J. Med. Chem.* **2004**, 47, 1879–1881; (d) Dayam, R.; Sanchez, T.; Neamati, N. *J. Med. Chem.* **2005**, 48, 9008–9015; (e) Barreca, M. L.; Ferro, S.; Rao, A.; De Luca, L.; Zappala, M.; Monforte, A.-M.; Debyser, Z.; Witvrouw, M.; Chimirri, A. *J. Med. Chem.* **2005**, 48, 7084–7088; (f) Dayam, R.; Sanchez, T.; Clement, O.; Shoemaker, R.; Sei, S.; Neamati, N. *J. Med. Chem.* **2005**, 48, 111–120; (g) Deng, J.; Lee, K. W.; Sanchez, T.; Cui, M.; Neamati, N.; Briggs, J. M. *J. Med. Chem.* **2005**, 48, 1496–1505; (h) Nair, V.; Chi, G.; Ptak, R.; Neamati, N. *J. Med. Chem.* **2006**, 49, 445–447; (i) Deng, J.; Sanchez, T.; Neamati, N.; Briggs, J. M. *J. Med. Chem.* **2006**, 49, 1684–1692; (j) Barreca, M. L.; De Luca, L.; Iraci, N.; Chimirri, A. *J. Med. Chem.* **2006**, 49, 3994–3997.
9. Warshel, A.; Levitt, M. *J. Mol. Biol.* **1976**, 103, 227–249.
10. Field, M. J.; Bash, P. A.; Karplus, M. *J. Comput. Chem.* **1990**, 11, 700–733.
11. Gao, J. *Acc. Chem. Res.* **1996**, 29, 298–305.
12. (a) Neamati, N. *Expert Opin. Ther. Pat.* **2002**, 12, 709–724; (b) Shionogi & Co. Ltd, W09950245-A, 1999; (c) Shionogi & Co. Ltd, W00117968-A, 2001.
13. Alves, C. N.; Martí, S.; Castillo, R.; Moliner, V.; Andrés, J.; Tuñón, I.; Silla, E. *Chem. Eur. J.*, **2007**, in press.
14. Alzate-Morales, J. H.; Contreras, R.; Soriano, A.; Tuñón, I.; Silla, E. *Biophys. J.* **2006**, 92, 430–439.
15. (a) Field, M. J. *A practical Introduction to the Simulation of Molecular Systems*; Cambridge University Press: Cambridge, U.K., 1999; (b) Field, M. J.; Albe, M.; Bret, C.; Proust-de Martin, F.; Thomas, A. *J. Comput. Chem.* **2000**, 21, 1088–1100.
16. Dewar, M. J. S.; Ziegler, E. G.; Healy, E. F.; Stewart, J. J. P. *J. Am. Chem. Soc.* **1985**, 107, 3902–3909.
17. Jorgensen, W. L.; Maxwell, D. S.; Tirado-Rives, J. *J. Am. Chem. Soc.* **1996**, 118, 11225–11236.
18. Jorgensen, W. L.; Chandrasekhar, J.; Madura, J. D.; Impey, R. W.; Klein, M. L. *J. Chem. Phys.* **1983**, 79, 926–935.
19. An overview of the *ab initio*/MM methodology used in this paper, albeit not explicitly stated, can be derived from references: (a) Zhang, Y.; Liu, H.; Yang, W. *J. Chem. Phys.* **2000**, 112, 3483–3492; (b) Martí, S.; Moliner, V.; Tuñón, I. *J. Chem. Theory Comput.* **2005**, 1, 1008–1016.
20. (a) Becke, A. D. *Phys. Rev. A* **1988**, 38, 3098–3100; (b) Lee, C.; Yang, W.; Parr, R. G. *Phys. Rev. B* **1988**, 37, 785–789.
21. (a) Jenkins, T. M.; Esposito, D.; Engelman, A.; Cragie, R. *EMBO J.* **1997**, 16, 6678–6849; (b) Eposito, D.; Cragie, R. *EMBO J.* **1998**, 17, 5832–5843; (c) Heuer, T. S.; Brown, P. O. *Biochemistry* **1997**, 36, 10655–10665; (d) Heuer, T. S.; Brown, P. O. *Biochemistry* **1998**, 37, 6667–6678.
22. Dougherty, D. A. *Science* **1996**, 271, 163–168.
23. Pommier, Y.; Johnson, A. A.; Marchand, C. *Nature* **2005**, 4, 236–248.
24. (a) Lameira, J.; Alves, C. N.; Moliner, V.; Silla, E. *J. Med. Chem.* **2006**, 41, 616–623; (b) Lameira, J.; Reis, M.; Medeiros, I. G.; Santos, A. S.; Alves, C. N. *Bioorg. Med. Chem.* **2006**, 41, 7105–7112; (c) Olivero-Verbel, J.; Pacheco-Londoño, L. *J. Chem. Inf. Comput. Sci.* **2002**, 42, 1241–1246.
25. GaussView, Version 3.0, Dennington II, Roy, Keith, Todd; Millam, John; Eppinnett, Ken; Hovell, W. Lee; and Gilliland, Ray; Semichem, Inc., Shawnee Mission, KS, 2003.
26. See the following references, where the method is explained and its accuracy compared with the one obtained with other methods: (a) Gilson, M. K. *Proteins Struct. Funct. Genet.* **1993**, 15, 266–282; (b) Antosiewicz, J.; McCammon, J. A.; Gilson, M. K. *J. Mol. Biol.* **1994**, 238, 415–436.
27. Field, M. J.; Amara, P.; David, L.; Rinaldo, D. personal communication.
28. Byrd, R. H.; Lu, P.; Nocedal, J.; Zhu, C. *J. Sci. Comput.* **1995**, 16, 1190–1208.
29. Breneman, C. M.; Wiberg, K. B. *J. Comput. Chem.* **1990**, 11, 361–373.